

# Supplementary Information

## **Attracted-Killed Inhibition Mechanism in Ag/Chitosan Hydrogel for Long-Acting Control of *Ralstonia solanacearum***

Yi-Hsin Chien<sup>a\*</sup>, Bo-Yan Lin<sup>a</sup>, Han-Hsiang Shih<sup>a</sup>, Chun-Yu Chen<sup>a</sup>, and Peng-Chieh Chen<sup>a</sup>

<sup>a</sup> Department of Materials Science and Engineering, Feng Chia University, Taichung, Taiwan

\*Corresponding author e-mail: [yhchien@fcu.edu.tw](mailto:yhchien@fcu.edu.tw)

**Table S1.** The summarized antimicrobial table includes antimicrobial materials, bacteria, monitoring methods, and antibacterial activity.

Type of antimicrobial materials	Test bacterial	Method	Antibacterial activity	Reference
TiO <sub>2</sub>	<i>E. coli</i>	Turbidity method	2.65 × 10 <sup>6</sup> UFC/mL	1
TiO <sub>2</sub>	<i>E. coli</i> and <i>S. aureus</i>	Disk diffusion	17.2mm和14.3mm	2
MgO	<i>E. coli</i> and <i>S. aureus</i>	Disk diffusion	12.7mm / 9.3mm (10 <sup>4</sup> CFU/mL <sup>-1</sup> )	3
Fe	<i>E. coli</i> / <i>S. aureus</i> / <i>P. aeruginosa</i>	Disk diffusion	27mm / 30mm / 29mm	4
FeO <sub>3</sub>	<i>Klebsiella pneumonia</i> and <i>Staphylococcus aureus</i>	Disk diffusion	42 和 47 mm (2.65 × 10 <sup>6</sup> UFC/mL)	5
Al <sub>2</sub> O <sub>3</sub>	<i>S. Pyogenes</i> and <i>P. vulgaris</i>	Disk diffusion	2.65 × 10 <sup>6</sup> UFC/mL	6
Ag	<i>E. coli</i> and <i>S. aureus</i>	Disk diffusion	9 mm / 9 mm	7
Ag	<i>E. coli</i> and <i>S. aureus</i>	Turbidity method and Disk diffusion	2.65 × 10 <sup>8</sup> UFC/mL	8
ZnO	<i>E. coli</i>	Agar dilution method	2.28 × 10 <sup>8</sup> UFC/mL	9
ZnO	<i>L. monocytogenes</i> and <i>E. coli</i>	Spread plate method	1 × 10 <sup>8</sup> CFU/mL	10
CuO	<i>P. aeruginosa</i> , <i>B. circulens</i> , <i>E. coli</i> and <i>S. sureus</i>	Turbidity method	10 <sup>7</sup> UFC/mL	11
CuO and ZnO	<i>P. aeruginosa</i> , <i>S. aureus</i> and <i>E. coli</i>	Disk diffusion	10 <sup>7</sup> UFC/mL	12
Cs/PVP	<i>E. coli</i> and <i>S. aureus</i>	Disk diffusion	25.53mm和15.40mm	13
Ag/CaO	<i>S. aureus</i>	Plate Count Agar	1 × 10 <sup>6</sup>	14
<b>Ag@Cs/Cs<sup>h</sup> hydrogel</b>	<b><i>R. solanacearum</i></b>	<b>Turbidity method</b>	<b>5x10<sup>8</sup> CFU/mL</b>	<b>This study</b>

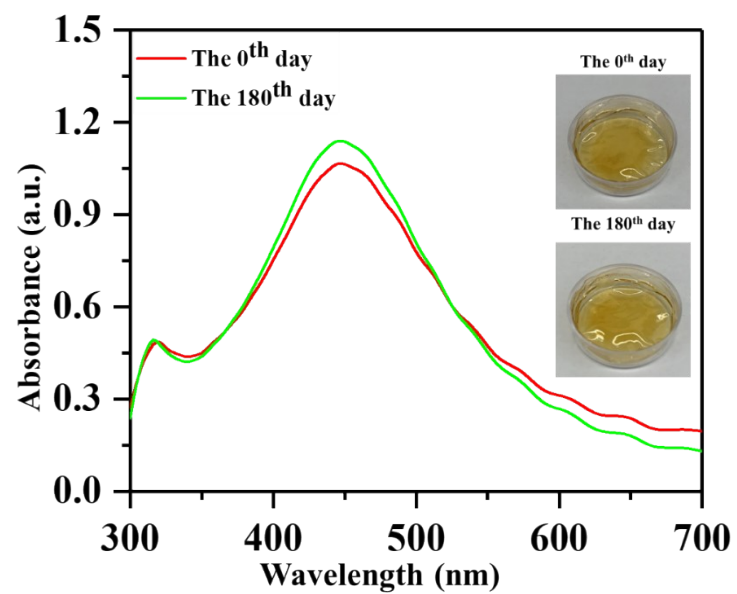
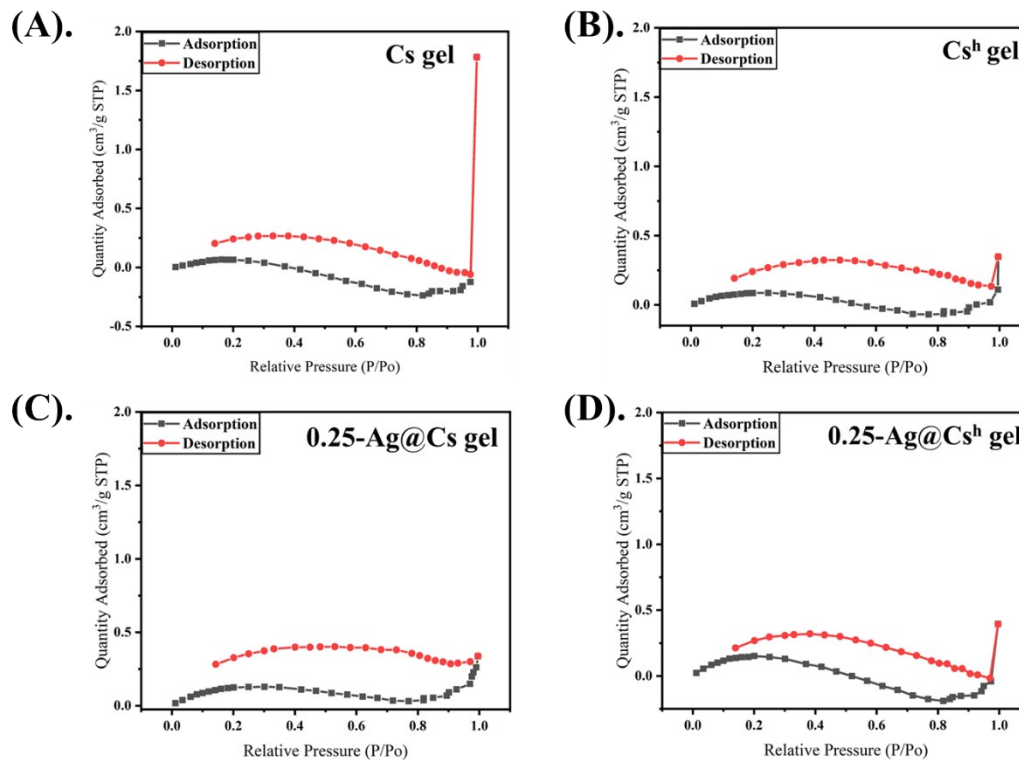


**Figure S1.** The stability test of 0.25-Ag@Cs gel through the optical property and morphology at the 180<sup>th</sup> using UV-Vis spectrum and photograph (insert).



(E).

Samples	Cs gel	Cs <sup>h</sup> gel	0.25-Ag@Cs gel	0.25-Ag@Cs <sup>h</sup> gel
Surface Area (m <sup>2</sup> /g)	0.5915	0.3722	0.5823	0.0165
Pore Volume (cm <sup>3</sup> /g)	0.000075	0.000170	0.000308	0.000203
Pore Size (Å)	5.0594	18.2191	21.1768	X

**Figure S2.** The N<sub>2</sub> adsorption/desorption isotherms of BET assay: (A). Cs gel; (B). Cs<sup>h</sup> gel; (C). 0.25-A@Cs gel; and (D) 0.25-A@Cs<sup>h</sup> gel. The BET profile, including surface area, pore volume, and pore size, is shown in (E).

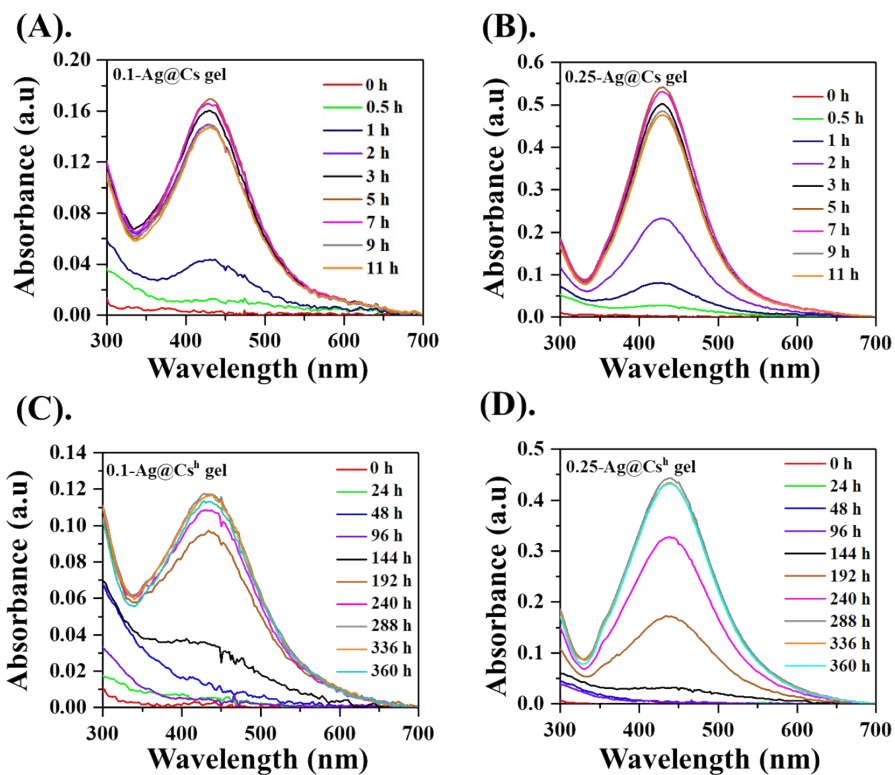


**Figure S3.** The absorbance peak at 434 nm was monitored by UV-Vis spectrum corresponding to the amount of Ag NPs released during water-soaking conditions: (A) 0.1-Ag@Cs gel; (B) 0.25-Ag@Cs gel; (C) 0.1-Ag@Cs<sup>h</sup> gel; (D) 0.25-Ag@Cs<sup>h</sup> gel.

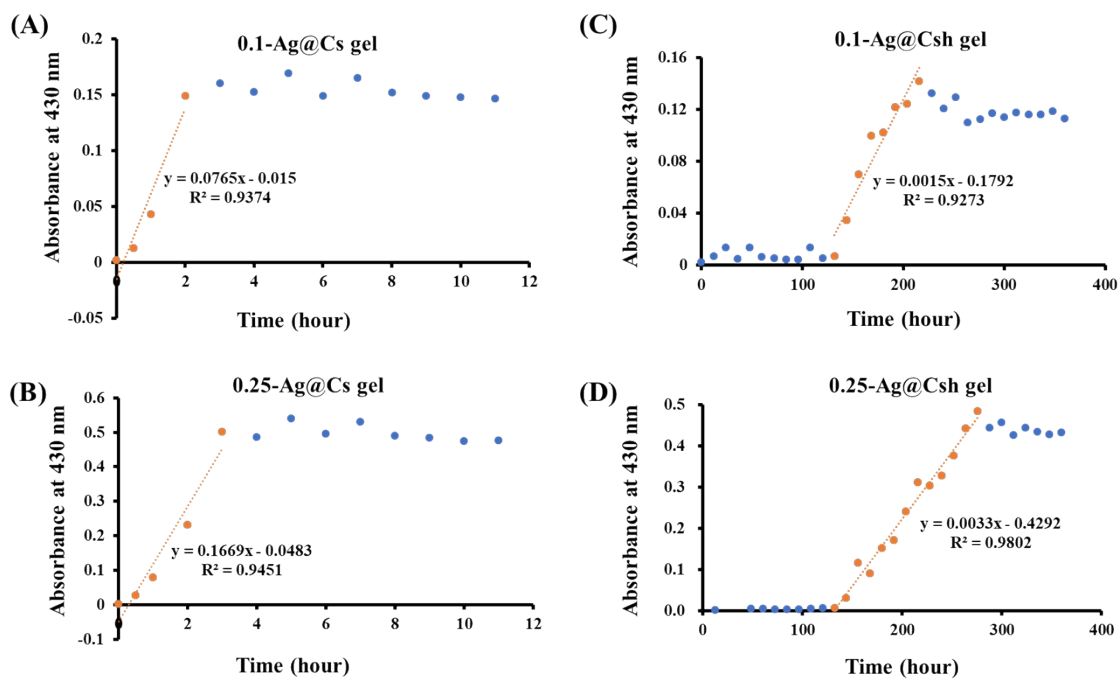


**Figure S4.** Ag NPs released versus time profile of Zero-order model in the partial time zone, indicating the absorption phase and elimination phase: (A) 0.1-Ag@Cs gel; (B) 0.25-Ag@Cs gel; (C) 0.1-Ag@Cs<sup>h</sup> gel; (D) 0.25-Ag@Cs<sup>h</sup> gel.

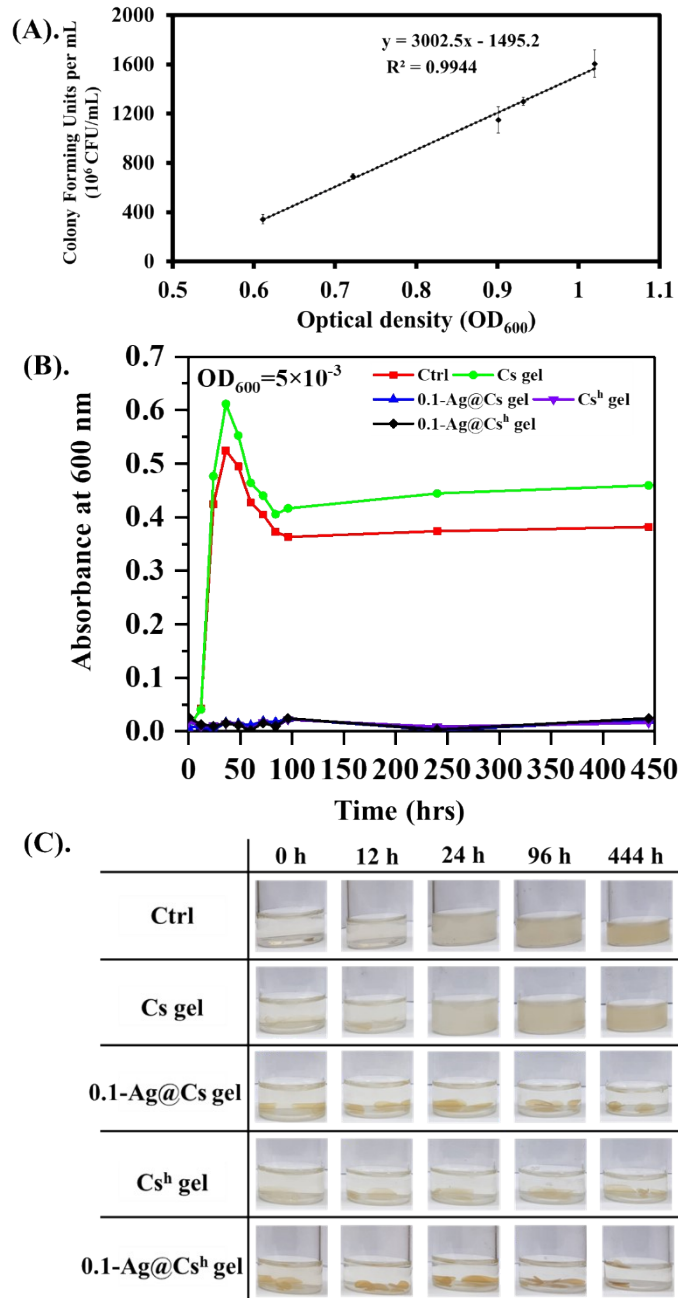


**Figure S5.** (A). The linear curve of *R. solanacearum* from  $3.2 \times 10^8$  CFU/mL to  $1.6 \times 10^9$  CFU/mL. Investigating sterilization ability in *R. solanacearum* concentration of  $5 \times 10^6$  CFU/mL with Cs/Cs<sup>h</sup> gel and 0.1/Ag@Cs/Cs<sup>h</sup> gel under 30 °C and 200 rpm incubator. (B). The intensity of  $OD_{600 \text{ nm}}$  was monitored using the UV-Vis spectrum; (C). The medium in the sample vials was observed to become turbid, indicating bacteria growth, as seen in the photographs of each condition.

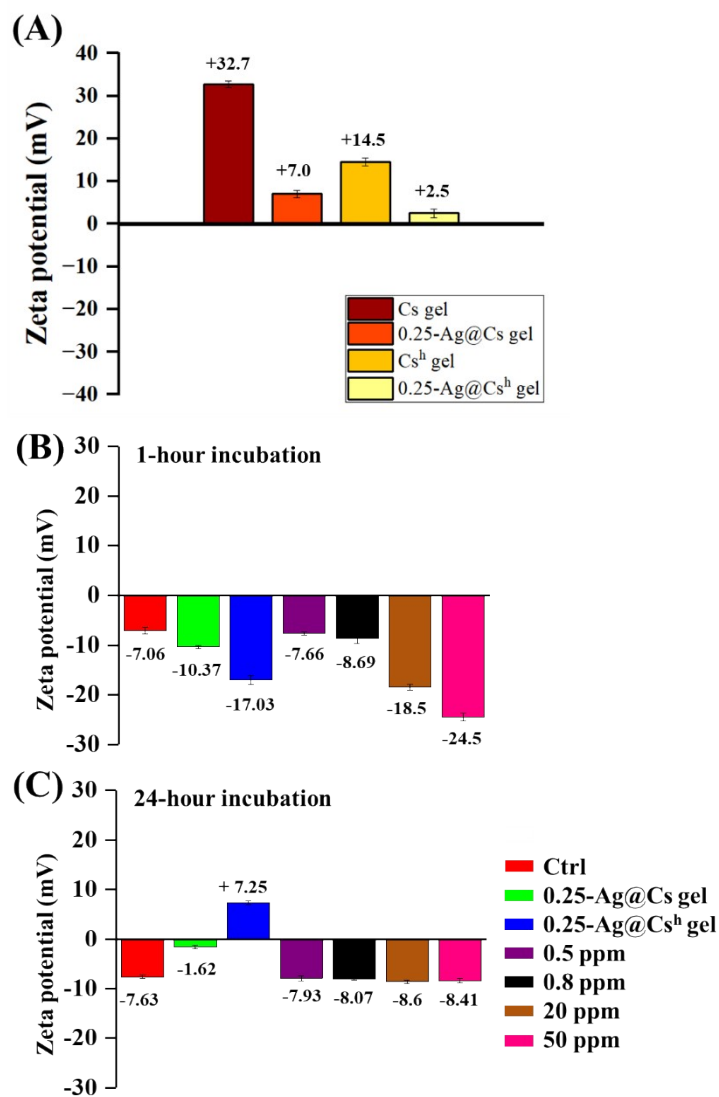


**Figure S6.** (A) The zeta potential profiles of Cs/Cs<sup>h</sup> gel and 0.25-Ag@Cs/Cs<sup>h</sup> gel in aqueous solution. The zeta potential profiles of Ctrl (*R. solanacearum*), 0.25-Ag@Cs/Cs<sup>h</sup> gel, 0.5, 0.8, 20, and 50 ppm were incubated with  $5 \times 10^8$  CFU/mL *R. solanacearum* for (B) 1-hour; (C) 24-hour incubation.



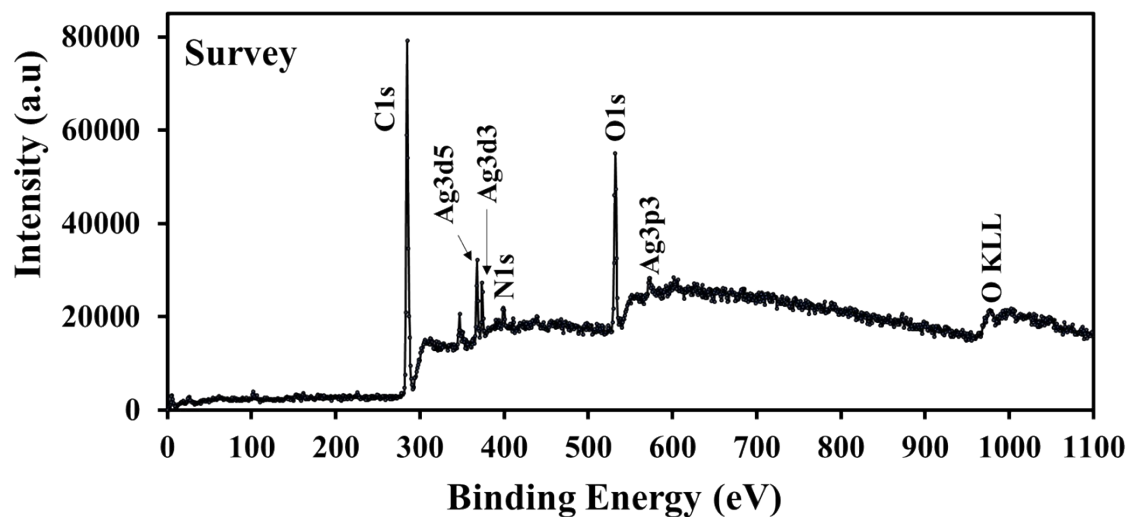


**Figure S7.** The XPS profiles of 0.25-Ag@Cs gel presented a full survey scan spectrum.

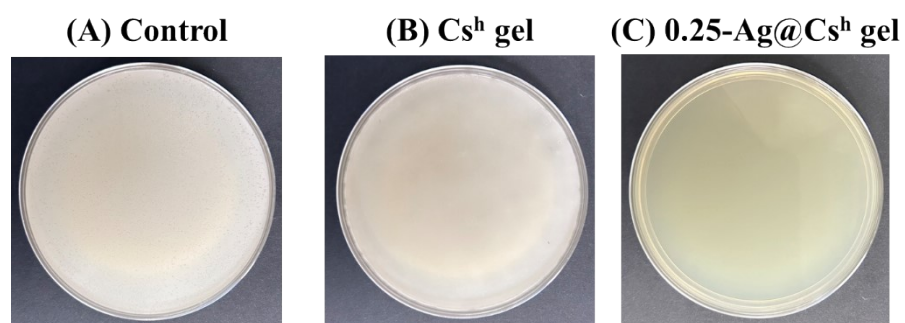


**Figure S8.** (A) The *R. solanacearum* concentration is  $5 \times 10^8$  CFU/mL as control; culture the sterilized *R. solanacearum* on agar plates: (B) Transferred 100  $\mu$ L of the solution from the Cs<sup>h</sup> gel mixture and (C) Transferred 100  $\mu$ L of the transparent solution from the 0.25-Ag@Cs<sup>h</sup> gel mixture for an additional 24 hours of culture under incubator at 30 °C.

## Reference

1. Vargas, Mónica Andrea, and Jorge E. Rodríguez-Páez. "Amorphous TiO<sub>2</sub> nanoparticles: Synthesis and antibacterial capacity." *Journal of Non-Crystalline Solids* 459 (2017): 192-205.
2. Anandgaonker, Priyanka, et., al. "Synthesis of TiO<sub>2</sub> nanoparticles by electrochemical method and their antibacterial application." *Arabian Journal of Chemistry* 12.8 (2019): 1815-1822.
3. Almontasser, A., A. Parveen, and A. Azam. "Synthesis, Characterization and antibacterial activity of Magnesium Oxide (MgO) nanoparticles." IOP Conference Series: Materials Science and Engineering. Vol. 577. No. 1. IOP Publishing, 2019.
4. Devatha, C. P., K. Jagadeesh, and Mallikarjun Patil. "Effect of Green synthesized iron nanoparticles by Azadirachta Indica in different proportions on antibacterial activity." *Environmental Nanotechnology, Monitoring & Management* 9 (2018): 85-94.
5. Abid, Muslim A., Duha A. Kadhim, and Wisam J. Aziz. "Iron oxide nanoparticle synthesis using trigonella and tomato extracts and their antibacterial activity." *Materials Technology* 37.8 (2022): 547-554.
6. Jawad, Anwar Sabri, Qasim N. Thewaini, and Sharafaldin Al-Musawi. "Cytotoxicity Effect and Antibacterial Activity of Al<sub>2</sub>O<sub>3</sub> Nanoparticles Activity against Streptococcus Pyogenes and Proteus Vulgaris." *Journal of Applied Sciences and Nanotechnology* 1.3 (2021): 42-50.
7. Ahmed, Shakeel, et., al. "Green synthesis of silver nanoparticles using Azadirachta indica aqueous leaf extract." *Journal of radiation research and applied sciences* 9.1 (2016): 1-7.
8. Biao, Linhai, et., al. "Synthesis, characterization and antibacterial study on the chitosan-functionalized Ag nanoparticles." *Materials Science and Engineering: C* 76 (2017): 73-80.
9. Chemingui, H., et., al. "Facile green synthesis of zinc oxide nanoparticles (ZnO NPs): Antibacterial and photocatalytic activities." *Materials Research Express* 6.10 (2019): 1050b4.
10. Kairyte, K., Kadys, A. & Luksiene, Z. Antibacterial and antifungal activity of photoactivated ZnO nanoparticles in suspension. *Journal of Photochemistry and Photobiology B* (2013) : Biology 128, 78- 84.
11. Das, Dhaneswar, et., al. "Synthesis and evaluation of antioxidant and antibacterial behavior of CuO nanoparticles." *Colloids and Surfaces B: Biointerfaces* 101 (2013): 430-433.

12. Dadi, Rania, *et al.* "Antibacterial activity of ZnO and CuO nanoparticles against gram positive and gram negative strains." *Materials Science and Engineering: C* 104 (2019): 109968.
13. . Tavakoli, Mohamadreza, *et., al.* "Fabrication and evaluation of Cs/PVP sponge containing platelet-rich fibrin as a wound healing accelerator: An in vitro and in vivo study." *International Journal of Biological Macromolecules* 204 (2022): 245-257.
14. Khan, Md Imran, *et., al.* "Biogenic Ag/CaO nanocomposites kill *Staphylococcus aureus* with reduced toxicity towards mammalian cells." *Colloids and Surfaces B: Biointerfaces* 189 (2020): 110846.